Geoscience Frontiers 8 (2017) 977–987

HOSTED BY

Contents lists available at ScienceDirect

China University of Geosciences (Beijing)

Geoscience Frontiers

journal homepage: www.elsevier.com/locate/gsf

Research paper

Meso–Cenozoic lithospheric thermal structure in the Bohai Bay Basin, eastern North China Craton

Zongxing Li [a], Yinhui Zuo [b,*], Nansheng Qiu [c], Jun Gao [d]

[a] The Key Laboratory of Shale Oil and Gas Geological Survey, Institute of Geomechanics, Chinese Academy of Geological Sciences, Beijing 100081, China
[b] State Key Laboratory of Oil and Gas Reservoir Geology and Exploitation, Chengdu University of Technology, Chengdu 610059, China
[c] State Key Laboratory of Petroleum Resource and Prospecting, China University of Petroleum, Beijing 102249, China
[d] Beijing Key Laboratory of Water Resources and Environment and Engineering, Chinese University of Geosciences, Beijing 100083, China

ARTICLE INFO

Article history:
Received 28 May 2016
Received in revised form
8 September 2016
Accepted 17 September 2016
Available online 1 October 2016

Keywords:
Bohai Bay Basin
Lithospheric thermal structure
Mesozoic
Moho temperature
North China Craton

ABSTRACT

The Bohai Bay Basin is a region where part of the North China Craton has been thinned and destroyed. It has experienced two periods of crustal thinning that occurred during the Cretaceous and Paleogene, but investigations of its Mesozoic and Cenozoic lithospheric thermal structure are limited. Therefore, in this study, the distributions of mantle heat flow, crustal heat flow, and Moho temperatures during the Meso–Cenozoic are calculated based on analyses of the thermal history of the Bohai Bay Basin. The results indicate that the ratio of mantle heat flow to surface heat flow peaked during the late stages of the early Cretaceous and during the middle to late Paleogene. The corresponding mantle heat flow was more than 65% of the surface heat flow. Moho temperatures reached three peaks: 900–1100 °C in the late stages of the early Cretaceous; 820–900 °C in the middle to late Paleogene; and (in the Linqing Depression, Cangxian Uplift, and Jizhong Depression) 770–810 °C during the early Neogene. These results reveal that the Bohai Bay Basin experienced significant geological change during the Cretaceous, including the transformation of lithospheric thermal structure from "cold mantle and hot crust" before the Cretaceous to "hot mantle and cold crust" after the Cretaceous. The results also indicate that the basin experienced two large-scale rifting events. Therefore, this work may provide the thermal parameters for further investigations of the geodynamic evolution of eastern China.

1. Introduction

The thermal structure of the lithosphere significantly impacts its thermal evolution. Research on lithospheric thermal structure focuses on surface heat flow, crustal structure, thermal physical parameters (e.g., heat production rate and thermal conductivity) of each layer, and the basic principles of heat transfer. These variables are used to analyze the composition of surface heat flow (including crustal and mantle heat flow), the distribution of heat flow in different layers, and deep lithospheric temperatures. Such investigations can reveal the structural relationships of crustal heat flow (i.e., heat generated by the decay of radioactive elements in the Earth's crust) and mantle heat flow (i.e., heat generated from the Earth's mantle up to the Moho), which help to constrain the causes of basin evolution and related geodynamics. Moreover, studying lithospheric thermal structure contributes to quantitative interpretations of terrestrial heat flow and to our understanding of lithospheric dynamics, rheological properties, and hydrocarbon generation. Types of lithospheric thermal structure are dependent on compositional properties and heat flow partitioning in the crust and mantle, and are also closely related to regional tectonic activity, especially mantle flow.

Lithospheric thermal structure refers to the compositional relationship and partitioning of heat flow between the crust and mantle (Blackwell, 1971). Crustal and mantle heat flow partitioning has implications for the present-day tectonic activity of the crust, upper mantle. Wang (1996) proposed the "cold crust and hot mantle" and "hot mantle and cold crust" concepts to explain the lithospheric thermal structure of basins. When crustal heat flow represents more than 50% of surface heat flow, the crust is considered to be relatively "hot", whereas the mantle is deemed relatively "cold", and the lithospheric thermal structure is

* Corresponding author.
E-mail address: zuoyinhui@tom.com (Y. Zuo).
Peer-review under responsibility of China University of Geosciences (Beijing).

http://dx.doi.org/10.1016/j.gsf.2016.09.003

described as “hot crust and cold mantle”. In the opposite scenario, the lithospheric thermal structure is classified as “cold crust and hot mantle”.

Lithospheric thermal structure has been studied worldwide since the late 1960s. Birch et al. (1968) first noted that surface heat flow is comprised of heat flow from the upper mantle and radiogenic heat flow from the radioactive decay of U, Th, and ^{40}K in the crust. Since the 1980s, lithospheric thermal structure has become a new focus of geodynamic research (Cermak and Bodri, 1986; Chen, 1988; Pasquale et al., 1990; Baumann and Rybach, 1992; McLennan and Taylor, 1996; Wang, 1996; Rudnick et al., 1998; Zang et al., 2002; Cooper et al., 2004; Gong et al., 2005; Liu et al., 2005; William et al., 2005; Nathan, 2006; Gornov et al., 2009; Mall and Sharma, 2009; Bruno, 2010; Ashchepkov et al., 2012; Wang and Cheng, 2012; Peng and Zou, 2013; Rao et al., 2013; Zuo et al., 2013; Jaupart and Mareschal, 2014; Qiu et al., 2014; He, 2015). The lithospheric thermal structure of Chinese basins has been studied extensively (e.g., Chen, 1988; Hu and Wang, 1994; Wang, 1996; Qiu, 1998; He et al., 2001; Gong et al., 2005; Liu et al., 2005; Rao et al., 2013; Zuo et al., 2013; Qiu et al., 2014; He, 2015). Wang (1996) suggested that the heat flow ratio between the crust and mantle is 1.37 in Northwest China and the type of lithospheric thermal structure is “cold mantle and hot crust”. However, Wang (1996) determined a crust–mantle heat flow ratio of 2.34 in Southwest China, with a “cold mantle and hot crust” type of lithospheric thermal structure. The central region of the Chinese continental lithosphere was found to have a crust–mantle heat flow ratio of 0.98, with a transitional-type lithospheric thermal structure (Wang, 1996). A crust–mantle heat flow ratio of 0.82 and a “hot mantle and cold crust” type of lithospheric thermal structure have been established for eastern China, and the lithosphere of southeastern China was found to have a crust–mantle heat flow ratio of 0.72, with a “hot mantle and cold crust” thermal structure (Wang, 1996). Qiu (1998) argued that the lithospheric thermal structure of China exhibits systematic changes from east to west, and that the proportion of mantle heat flow decreases from the Liaohe Basin to the Tarim Basin. The heat flow from areas that were tectonically active and from the deep mantle is generally large, particularly from the Meso–Cenozoic rift basins of eastern China. However, heat flow from the deep mantle is low in tectonically stable regions, including western China.

The post-Mesozoic geodynamic evolution of Chinese continental lithosphere is mainly characterized by thickening in the west and thinning in the east (Zuo et al., 2015). Evidence of lithospheric thinning in eastern China is provided by studies of mantle xenoliths, igneous petrology, igneous geochemistry, structural geology, geophysics, and geothermal geology (Chen, 2009; Xu and Zhao, 2009; Li et al., 2012a,b, 2013; Zhu et al., 2012; Zuo et al., 2013; Qiu et al., 2014; He, 2015; Dmitrienko et al., 2016; Liu et al., 2016). It is also evident from the Mesozoic and Cenozoic rift basins, Qinling–Dabie orogenic belts, and intra-continental deep subduction zones. The Bohai Bay Basin is not only the center of lithospheric thinning in the eastern part of the North China Craton, but also contains abundant oil and gas. Moreover, the lithosphere of the Bohai Bay Basin experienced two stages of thinning, in the Cretaceous and Paleogene (Zuo et al., 2013; Qiu et al., 2014, 2015a,b; He, 2015).

Previous studies have focused on the present-day lithospheric thermal structure of the Bohai Bay Basin. In general, the results suggest that mantle heat flow accounted for 49–62% of the surface heat flow (Chen, 1988; Wang, 1996; Qiu, 1998; Gong, 2003, 2005). The contribution of mantle heat flow to surface heat flow in the Bohai Bay Basin is greater than the global average of 46% (Wang, 1996). However, investigations of Meso–Cenozoic lithospheric thermal structure are relatively scarce. Therefore, based on the thermal history of the Bohai Bay Basin during the Mesozoic and Cenozoic (Zuo et al., 2011, 2013, 2015; Qiu et al., 2014, 2015a,b), we calculated the crustal and mantle heat flow partitioning and the Moho temperature of the Bohai Bay Basin in different geological periods using the one-dimensional, steady-state, heat conduction equation, and then investigated the Meso–Cenozoic lithospheric thermal structure of the basin. This work provides thermal parameters for further research into the dynamic evolution of the continental lithosphere of eastern China, and also provides important insight into the tectonic evolution of the Bohai Bay Basin.

2. Geological setting

2.1. Tectonic evolution

The Bohai Bay Basin is a Meso–Cenozoic continental rift basin with an area of approximately 200,000 km^2 that developed on Archean–Paleoproterozoic crystalline basement. The basin is bounded by the Jiaodong uplift to the east, Taihangshan Mountain fault zone to the west, Yanshanian orogenic belt to the north, and Luxi Uplift to the south. It is comprised of the Liaohe, Bozhong, Jiyang, Huanghua, Jizhong, and Linqing depressions, as well as the Cangxian, Chengning, and Neihuang uplifts (Fig. 1). The basin contains Paleozoic to Cenozoic strata. The Cenozoic strata include the Kongdian, Shahejie, Dongying, Guantao, Minghuazhen, and Pingyuan formations (Fig. 2). Since the middle Proterozoic, the Bohai Bay Basin has experienced four main phases of tectonic evolution (Tian et al., 2000; Hou et al., 2001). The first phase was one of tectonic stability and sedimentation that lasted from the middle–late Proterozoic to the end of the Paleozoic, during which the Bohai Bay Basin had a “cool” lithosphere with a thickness of up to 200 km (Wu et al., 2007; Zhang and Yang, 2007). The second phase was characterized by uplift and folding during the Mesozoic, when most of basin was uplifted as a result of Hercynian tectonism in the late Permian. From the late Jurassic to the early Cretaceous, the Bohai Bay Basin underwent significant rifting due to the subduction of the Pacific Plate beneath the Eurasian Plate and the resultant upwelling of asthenospheric mantle. A thick sequence of clastic rocks was deposited in the basin, which also experienced silicic magmatism. The lithospheric thickness was reduced to 51–61 km during this period (Zuo et al., 2013; Qiu et al., 2014, 2015a,b). The Bohai Bay Basin then underwent thermal subsidence in the late Cretaceous. The third phase in the tectonic evolution of the basin was a syn-rift period that occurred in the Paleogene. The basin developed episodically, beginning with early syn-rift deposition of the Kongdian to Shahejie 4 formations, followed by significant rifting and deposition of the Shahejie 3 Formation, and the late syn-rift deposition of the Shahejie 1 to Dongying formations. The fourth evolutionary phase of the Bohai Bay Basin is defined by regional thermal subsidence from the Neogene to the Quaternary.

2.2. Crustal and lithospheric structure

The Moho beneath the Bohai Bay Basin is 28–36 km deep. The shallowest Moho depth of ~28 km depth occurs beneath the Bozhong depression, and crustal thickness gradually increases toward the surrounding orogenic belts. Moho uplift is also evident beneath the Jizhong depression, where the Moho depth is 32–35 km. Elsewhere in the basin, Moho depths range from 30 to 36 km (Liu, 1987; Wu et al., 2007) (Fig. 3). The present-day lithosphere of the Bohai Bay Basin is 60–120 km thick, according to seismic migration techniques (Chen et al., 2006, 2008; Chen, 2009; Zhu et al., 2011), and 76–102 km thick, according to thermochronology (Qiu et al., 2015a,b).

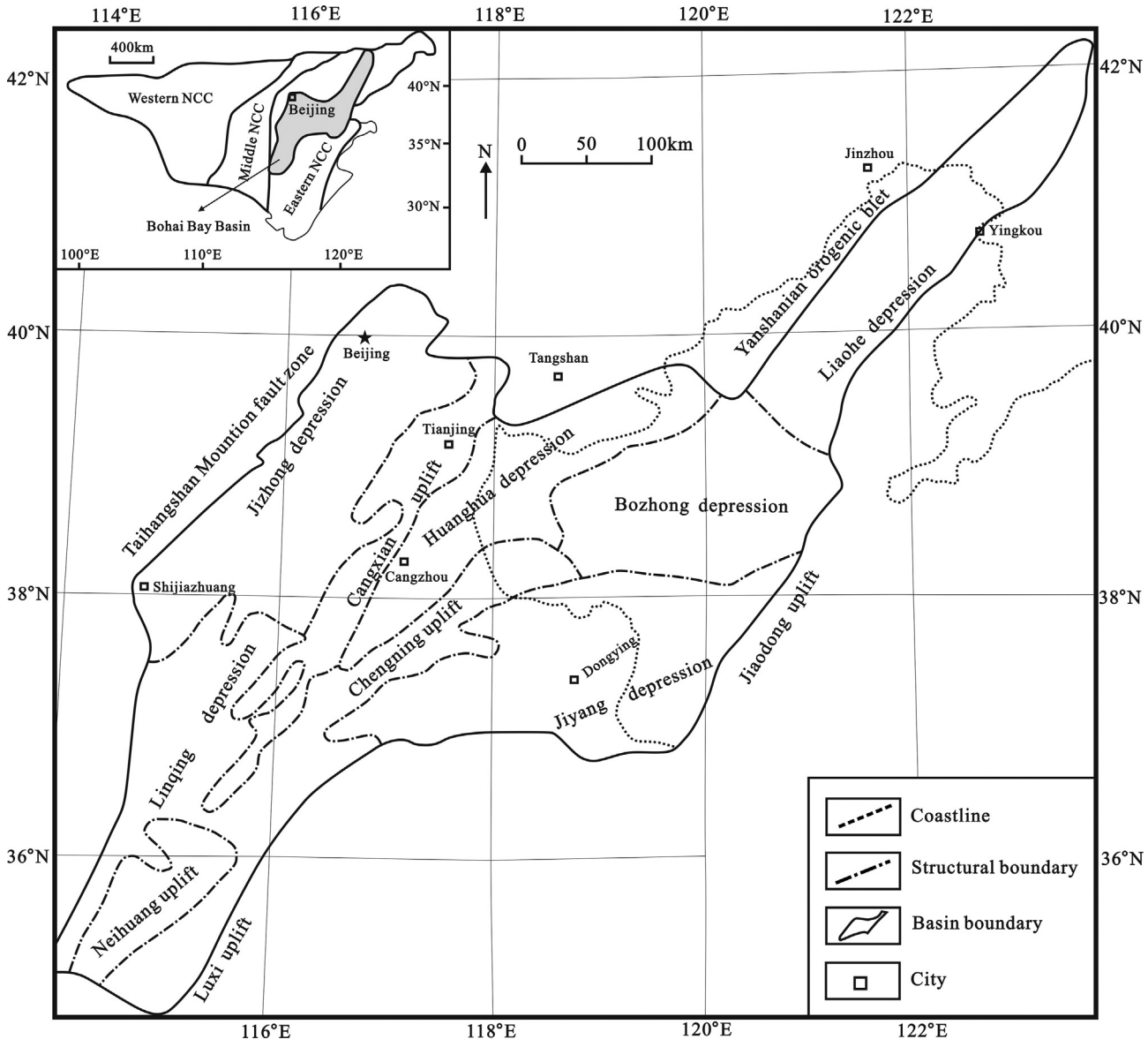

Figure 1. Structural units in the Bohai Bay Basin.

3. Methodology for calculating lithospheric thermal structure

Using a stepped function equation (Eq. 1), the top and bottom heat flows were calculated for each crustal layer in different geological periods. After determining the paleo-surface heat flow, the heat flow partitioning between each crustal layer and the mantle was obtained. Then, a lithospheric geothermal gradient with depth was calculated based on the one-dimensional, steady-state, heat conduction equation (Eq. 2).

$$q_0(t) = q_m(t) + \sum A_i(t)Z_i(t) \quad (1)$$

where $q_0(t)$ is surface heat flow in a given geological period, in mW/m^2; $q_m(t)$ is mantle heat flow in a given geological period, in mW/m^2; i is the number of structural layers; $A_i(t)$ is the radioactive heat production rate of the ith layer in a given geological period, in μW/m^3; and $Z_i(t)$ is the thickness of the ith layer in a given geological period, in km.

$$T_i^b(t) = T_i^t(t) + \left[q_i^t(t) \times Z_i(t)\right]/K_i - \left[A_i(i) \times Z_i^2(t)\right] \Big/ \left[2 \times K_i(t)\right] \quad (2)$$

where i, $Z_i(t)$, and $A_i(t)$ are the same as in Eq. (1); $T_i^t(t)$ and $T_i^b(t)$ are the top and bottom surface temperatures for the ith layer in a given geological period, respectively, in °C; $q_i(t)$ is heat flow of the top of the ith layer in a given geological period, in mW/m^2; and $K_i(t)$ is the thermal conductivity of the ith layer in a given geological period, in W/(m·K).

4. General parameters

4.1. Geological parameters

Geological parameters, including stratigraphic data, crustal thickness, lithological data, and stratigraphic ages, are necessary for calculating the crustal and mantle heat flows and deep lithospheric temperatures in different geological periods. The basal ages of the

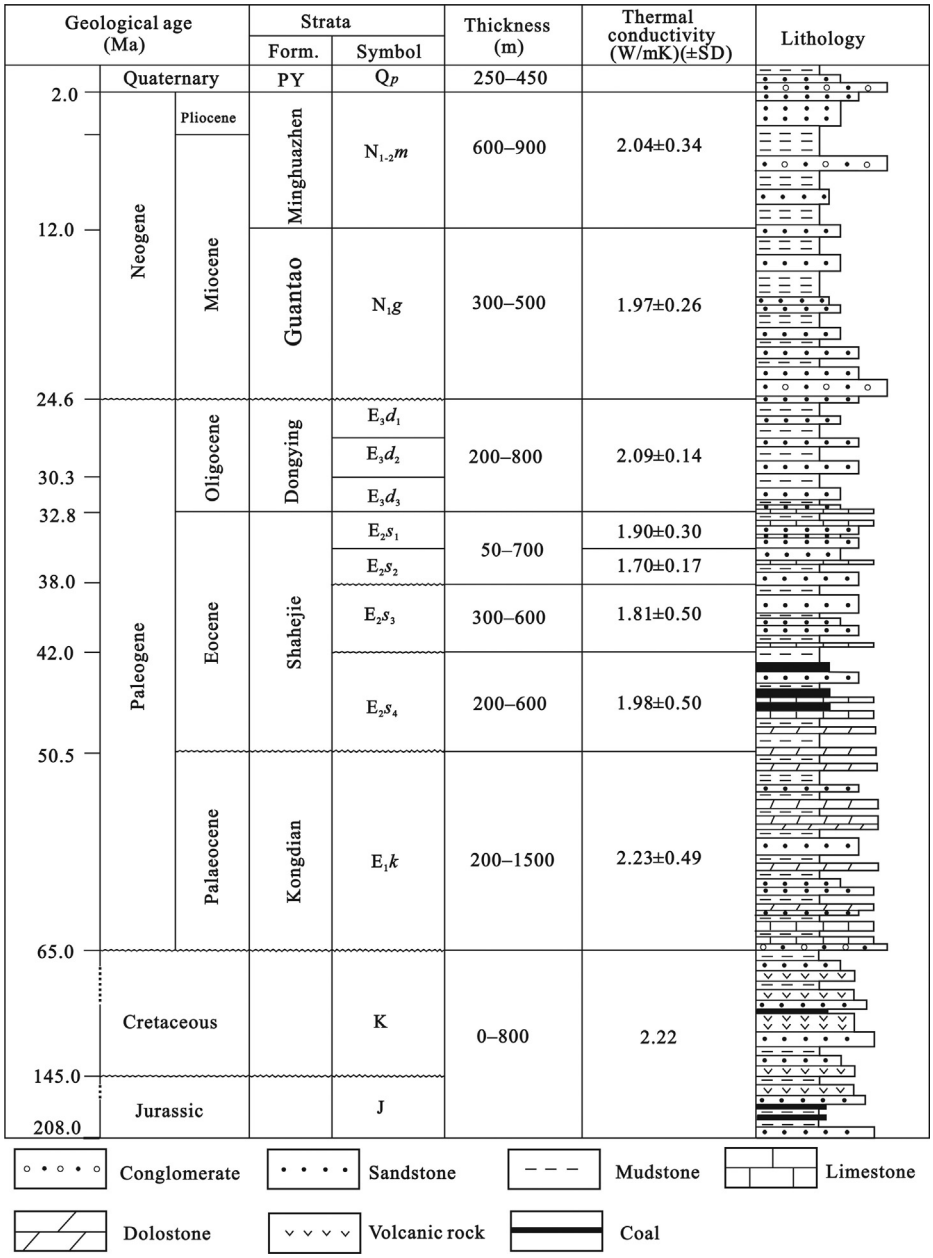

Figure 2. Stratigraphic column in the Bohai Bay Basin. Form. = Formation; PY = Pingyuan. Thermal conductivity is shown as mean value ± SD previous studies (Gong, 2003), where SD is standard deviation.

stratigraphic units of interest are as follows: 2.0 Ma for Quaternary strata; 5.1 Ma for the Neogene Minghuazhen Formation; 24.6 Ma for the Neogene Guantao Formation; 32.8 Ma for the Oligocene Dongying Formation; 50.5 Ma for the Eocene Shahejie Formation; 32.8 Ma for the Paleocene Kongdian Formation; 145 Ma for Cretaceous strata; 208 Ma for Jurassic strata; and 245 Ma for Triassic strata. The stratigraphic and lithological data are from borehole analyses. Regional stratigraphic information is extrapolated in areas lacking boreholes that intersect Mesozoic and Paleozoic strata (Chen, 1988; Ji et al., 2006). The structure and thickness of the crust during the key geological periods are presented in Fig. 3.

4.2. Thermal physical parameters

Thermal physical parameters of rocks include heat production rate (A) and thermal conductivity (K). The heat production rates for the sedimentary cover rocks were taken from previous studies (Table 1). The heat production rates of the crust beneath the sedimentary cover strata were calculated using the exponential decay model (Eq. 3).

$$A = A_0^{(-Z/D)} \tag{3}$$

where D is the depth scaling parameter for the heat producing layer; and A_0 is the heat production rate of near-surface rocks (1.24 μW/m^3; Liu et al., 2005).

However, Ketcham (1996) suggested that this model cannot be used throughout the crust because it underestimates the heat production of the middle and upper crust. Therefore, we assume that the exponential model of radiogenic heat production distribution can only be used in the upper crust, and heat production rates in the middle and lower crusts are considered to be constant at 0.86 and 0.31 μW/m^3, respectively (Liu et al., 2005). The mantle

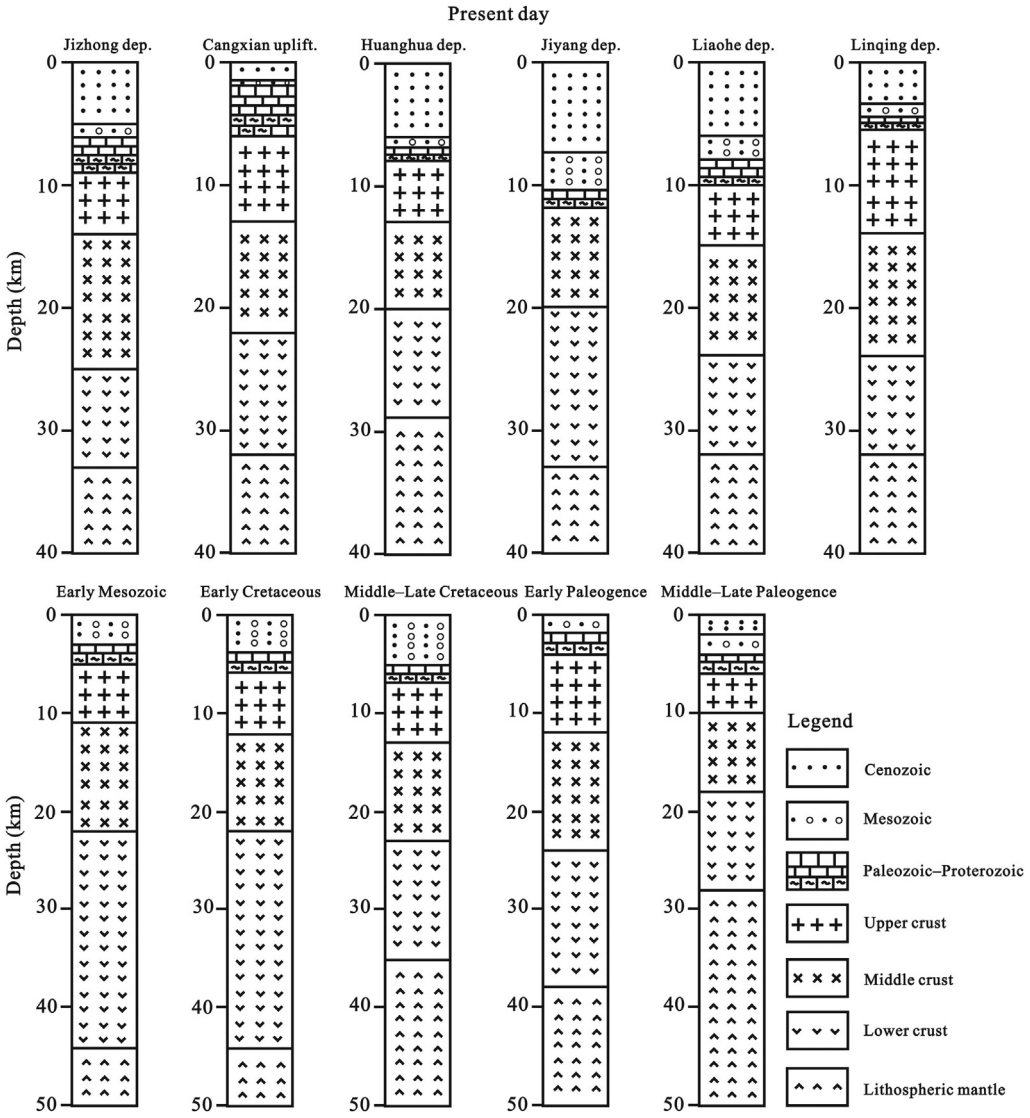

Figure 3. Crust model layers of the main structural units in the Bohai Bay Basin. The present-day crustal layers referred to literature (Cai et al., 2007). The crusted layers in the main geological history were speculated on the basis of the previous results of Petrology, Petrogeochemistry and tectonic evolution in this region (Shao et al., 2005; Wu et al., 2005a,b; Zhai et al., 2005; Zhu et al., 2008).

heat production rate is also assumed to be constant at 0.03 μW/m^3 (Rudnick et al., 1998).

The thermal conductivity values of the sedimentary cover rocks are adopted from previously published values (Chen, 1988; Gong, 2003; Liu et al., 2005) (Table 1). However, the thermal conductivity of the lower crust cannot be directly measured, and the value of each layer must be obtained from the K–T relationship (Eq. 4).

$$K = K_0 = (1 + cT)^{-1} \quad (4)$$

where K_0 is the initial thermal conductivity of the top surface of each structural layer, in W/(m·K); and c is the dimensionless thermal effect coefficient.

For the upper crust, middle crust, lower crust, and mantle, K_0 is 2.3, 2.5, 2.5 and 3.4 W/(m·K), respectively (Rudnick et al., 1998), and c is 0.001, 0, 0 and −0.00025, respectively. The surface temperature was set to 15 °C, and the heat production rate ($A_i(t)$) and the thermal conductivity ($K_i(t)$) of each structural layer were obtained using present-day values during the geological periods of interest.

4.3. Paleo-surface heat flow parameters

Paleo-heat flow data from the Bohai Bay Basin provide important parameters for our models. These values were obtained from vitrinite reflectance (R_o) and apatite fission track (AFT) data (Zuo et al., 2011, 2013, 2015; Qiu et al., 2014, 2015a,b), which are commonly used to reconstruct thermal histories of sedimentary basins (Sweeney and Burnham, 1990; Lerche, 1998; Hu et al., 2001; Qiu et al., 2014, 2015a,b; Zuo et al., 2015, 2016).

R_o data from nearly 200 wells and AFT data from Cenozoic samples from wells Jinqian 5, Jinqian 7, Yang 8, Qikou 17-9-3, Bozhong 25-1-1, and Bozhong 28-2-1 were collected to enable reconstruction of the Cenozoic thermal history (Zuo et al., 2013). Thermal indicators that can reliably record Mesozoic thermal information must be used to decipher the Mesozoic thermal history. Most areas of the Bohai Bay Basin contain Cenozoic strata that are thousands of meters thick. Most Mesozoic strata were deeply buried, resulting in resetting of AFT ages, such that they cannot be used to reconstruct the Mesozoic thermal history. The partial annealing zone of apatite may have been attained in several wells

Table 1
Rock heat production rate and thermal conductivity of each tectonic layer in the Bohai Bay Basin.

Structural layer	Rock heat generation ($\mu W/m^3$)	Rock thermal conductivity (W/m K)
Cenozoic	0.80	1.6
Mesozoic	1.26	2.0
Paleozoic	0.97	3.0
Upper crust	1.24	2.3
Middle crust	0.86	2.5
Lower crust	0.31	2.5
Lithospheric mantle	0.03	3.4

in depressions. However, the Mesozoic thermal history is more likely to be recorded by thermal indicators from wells where significant erosion occurred due to tectonic uplift at the end of the Mesozoic and/or Cenozoic. Accordingly, thermal indicator data from 12 wells were used to constrain the Mesozoic thermal history. Furthermore, samples from three wells that intersected the Mesozoic strata were chosen for the AFT test (Zuo et al., 2013). During modeling, the Easy%R_o model of R_o (Sweeney and Burnham, 1990) and the fan model of AFT annealing (Laslett et al., 1987) were applied.

The results show that the Bohai Bay Basin experienced the Mesozoic and Cenozoic heat flow peaks (Table 2) and experienced five thermal stages, as follows: (1) a stage of low and stable heat flow from the Triassic to Jurassic, with a heat flow of 53–58 mW/m^2; (2) a heat flow peak from the early Cretaceous to the middle of the late Cretaceous, with a maximum heat flow of 81–87 mW/m^2; (3) post-rift thermal subsidence from the middle of the late Cretaceous to the Paleocene, with a heat flow of 65–74 mW/m^2 at the end of the Cretaceous; (4) a second heat flow peak from the Eocene to Oligocene, with a maximum heat flow of 81–88 mW/m^2; and (5) a second stage of thermal subsidence from the Neogene to present, with an average heat flow of 64 mW/m^2 (Fig. 4).

5. Results

Crustal and mantle heat flows and Moho temperatures were calculated for every 5 Myr using the methodology described above (Tables 3–8).

5.1. Meso–Cenozoic crustal and mantle heat flow partitioning

The Meso–Cenozoic ratio of mantle heat flow to surface heat flow experienced two main increases and decreases in the Bohai Bay Basin. During the Triassic and Jurassic, the basin had low crustal and mantle heat flows under compressive tectonic stress. Therefore, the ratio of mantle heat flow to surface heat flow was less than

Table 2
The maximum palaeo-surface heat flow of the Bohai Bay Basin in the main geologic periods.

Structural units	Maximum palaeo-surface heat flow (mW/m^2)	
	Mesozoic	Cenozoic
Linqing depression	84.54	84.33
Cangxian uplift	81.67	87.67
Jizhong depression	85.97	80.82
Jiyang depression	86.08	87.30
Huanghua depression	82.52	83.26
Liaohe depression	80.62	87.67

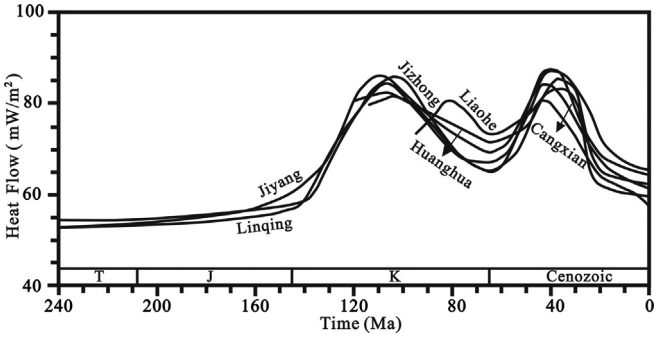

Figure 4. Meso–Cenozoic thermal history in the Bohai Bay Basin.

50%. The Bohai Bay Basin had a “cold mantle and hot crust” type of lithospheric thermal structure. Compressive tectonic stress evolved into a tensile stress regime beginning in the Cretaceous, and the surface and mantle heat flow rapidly increased. The ratio of mantle heat flow to surface heat flow surpassed 50%, reaching an initial peak of 63–68% in the middle to late Cretaceous. During this period, the Bohai Bay Basin had a “hot mantle and cold crust” type of lithospheric thermal structure. The stress regime changed again, this time to compressive tectonic stress during the late Cretaceous. Both surface and mantle heat flows decreased, but the ratio of mantle heat flow to surface heat flow remained above 50%. In addition, the basin retained a “hot mantle and cold crust” type of lithospheric thermal structure. Both surface and mantle heat flows increased again beginning in the Paleogene, and the ratio of mantle heat flow to surface heat flow reached a second peak of 73–75% in the middle to late Paleogene. During this period, the Bohai Bay Basin still had a “hot mantle and cold crust” type of lithospheric thermal structure. The basin underwent thermal subsidence beginning in the Neogene, and the ratio of mantle heat flow to surface heat flow decreased again to 53–61%, which is consistent with the results of previous studies (Wang, 1996; Gong et al., 2005; Liu et al., 2005; He, 2015). During this phase, the Bohai Bay Basin had a “hot mantle and cold crust” type of lithospheric thermal structure (Fig. 5).

5.2. Meso–Cenozoic Moho temperatures

Moho temperature depends on the surface heat flow, geothermal gradient, thermal physical parameters (heat production rate and thermal conductivity), and thicknesses of crustal layers.

The evolution of Moho temperatures was similar in each tectonic unit in the Bohai Bay Basin. Beginning in the Mesozoic, Moho temperatures reached more than 600 °C and peaked three times, in the late stages of the early Cretaceous, middle to late Paleogene, and early Neogene (Fig. 6). Moho temperatures rapidly increased during the Cretaceous, peaking in the late stages of the early Cretaceous at a temperature of 900–1100 °C. Moho temperatures then gradually decreased to 720–820 °C at the end of the Cretaceous. The basin underwent rifting and lithospheric thinning during the Paleogene. Moho temperatures increased again, attaining a second peak at 820–900 °C during the middle to late Paleogene. The basin then experienced thermal subsidence during the Neogene, and Moho temperatures peaked a third time, but only in the Linqing Depression, Cangxian Uplift, and Jizhong Depression. However, the maximum temperature was significantly lower than those of the previous two thermal peaks. Moho temperatures subsequently decreased to 640–780 °C, where it remains today.

Table 3
Moho temperatures and heat flow partition of the Jiyang Depression during the Mesozoic and Cenozoic.

Time (Ma)	T_m (°C)	q_0 (mW/m^2)	q_m (mW/m^2)	q_c (mW/m^2)	q_m/q_0
240	617.8	52.96	24.39	28.57	46.0%
235	621.6	53.18	24.61	28.57	46.3%
230	622.5	53.23	24.66	28.57	46.3%
225	625.3	53.39	24.82	28.57	46.5%
220	626.2	53.44	24.87	28.57	46.5%
215	628.1	53.55	24.98	28.57	46.6%
210	630.9	53.71	24.97	28.73	46.5%
205	635.5	53.97	25.17	28.80	46.6%
200	638.2	54.13	25.33	28.81	46.8%
195	643.0	54.40	25.45	28.95	46.8%
190	646.6	54.61	25.70	28.91	47.1%
185	652.2	54.93	26.01	28.92	47.4%
180	655.9	55.14	26.11	29.03	47.4%
175	664.3	55.62	26.41	29.20	47.5%
170	668.8	55.88	26.54	29.34	47.5%
165	679.1	56.47	26.98	29.49	47.8%
160	690.1	57.10	27.36	29.74	47.9%
155	706.9	58.06	27.98	30.07	48.2%
150	708.0	59.23	28.71	30.51	48.5%
145	712.0	60.61	29.64	30.96	48.9%
140	720.0	62.57	31.40	31.17	50.2%
135	749.9	65.12	33.97	31.15	52.2%
130	774.4	68.35	38.15	30.20	55.8%
125	864.2	74.24	44.04	30.20	59.3%
120	928.5	80.66	52.94	27.72	65.6%
115	948.3	84.54	56.82	27.72	67.2%
110	1006.4	86.08	58.36	27.72	67.8%
105	993.5	85.18	57.46	27.72	67.5%
100	956.8	82.63	54.91	27.72	66.5%
95	920.9	80.13	52.41	27.72	65.4%
90	925.7	77.75	48.21	29.54	62.0%
85	829.3	75.57	46.03	29.54	60.9%
80	860.6	73.50	43.96	29.54	59.8%
75	837.0	71.96	42.42	29.54	58.9%
70	813.4	70.42	40.88	29.54	58.0%
65	766.9	69.31	40.94	28.37	59.1%
60	783.0	70.42	42.05	28.37	59.7%
55	829.3	73.61	45.24	28.37	61.5%
50	905.5	78.86	50.49	28.37	64.0%
45	832.8	84.06	62.33	21.73	74.1%
40	869.8	87.30	65.57	21.73	75.1%
35	861.9	86.61	64.88	21.73	74.9%
30	829.1	83.74	62.01	21.73	74.0%
25	820.0	79.28	52.54	26.74	66.3%
20	810.0	72.76	46.02	26.74	63.3%
15	806.0	69.31	42.57	26.74	61.4%
10	804.9	67.34	40.60	26.74	60.3%
5	787.5	66.18	39.44	26.74	59.6%
0	777.2	65.49	38.75	26.74	59.2%

T_m–Moho temperatures, °C; q_0–surface heat flow, mW/m^2; q_m–mantle heat flow, mW/m^2; q_c–crustal heat flow, mW/m^2; q_m/q_0–Ratio of the mantle heat flow to surface heat flow, %.

Table 4
Moho temperatures and heat flow partition of the Linqing Depression during the Mesozoic and Cenozoic.

Time (Ma)	T_m (°C)	q_0 (mW/m^2)	q_m (mW/m^2)	q_c (mW/m^2)	q_m/q_0
240	616.1	52.86	24.29	28.57	46.0%
235	616.1	52.86	24.29	28.57	46.0%
230	617.8	52.96	24.39	28.57	46.0%
225	620.6	53.12	24.55	28.57	46.2%
220	621.6	53.18	24.61	28.57	46.3%
215	624.4	53.34	24.77	28.57	46.4%
210	623.4	53.28	24.71	28.57	46.4%
205	627.1	53.49	24.92	28.57	46.6%
200	629.0	53.60	25.03	28.57	46.7%
195	631.0	53.71	25.14	28.57	46.8%
190	631.8	53.76	25.19	28.57	46.9%
185	635.3	53.92	25.39	28.53	47.1%
180	638.2	54.13	25.56	28.57	47.2%
175	641.9	54.34	25.77	28.57	47.4%
170	646.6	54.61	26.04	28.57	47.7%
165	652.2	54.93	26.36	28.57	48.0%
160	658.7	55.30	26.7	28.60	48.3%
155	665.2	55.67	27.1	28.57	48.7%
150	675.3	56.25	27.68	28.57	49.2%
145	688.4	57.00	28.43	28.57	49.9%
140	724.6	59.07	30.5	28.57	51.0%
135	728.6	63.79	32.42	31.37	52.0%
130	785.0	69.04	38.84	30.20	56.3%
125	852.2	73.45	43.25	30.20	58.9%
120	879.8	77.27	49.55	27.72	64.1%
115	926.3	80.51	52.79	27.72	65.6%
110	970.5	83.58	55.86	27.72	66.8%
107	984.3	84.54	56.82	27.72	67.2%
105	979.7	84.22	56.5	27.72	67.1%
100	940.4	81.94	53.77	28.17	65.6%
95	901.0	78.75	51.03	27.72	64.8%
90	894.7	75.73	46.19	29.54	61.0%
85	845.1	72.49	42.95	29.54	59.2%
80	802.9	69.73	40.19	29.54	57.6%
75	773.6	67.82	38.28	29.54	56.4%
70	766.3	67.34	37.8	29.54	56.1%
65	736.9	67.24	38.87	28.37	57.8%
60	753.0	68.35	39.98	28.37	58.5%
55	800.0	71.59	43.22	28.37	60.4%
50	880.0	77.11	48.74	28.37	63.2%
45	823.7	83.26	61.53	21.73	73.9%
43	835.9	84.33	62.6	21.73	74.2%
40	834.1	84.17	62.44	21.73	74.2%
35	799.0	81.09	59.36	21.73	73.2%
30	746.8	76.53	54.8	21.73	71.6%
25	870.3	71.70	44.96	26.74	62.7%
20	813.0	67.88	41.14	26.74	60.6%
15	774.0	65.28	38.54	26.74	59.0%
10	752.4	63.84	37.1	26.74	58.1%
5	731.7	62.46	35.72	26.74	57.2%
0	702.1	61.45	35.85	25.60	56.0%

T_m, q_0, q_m, q_c and q_m/q_0 are referred to Table 2.

6. Discussion

6.1. Differences in Meso–Cenozoic crustal and mantle heat flow partitioning and Moho temperature evolution between tectonic units of the Bohai Bay Basin

There are differences in the Meso–Cenozoic crustal and mantle heat flow evolution between different tectonic units in the Bohai Bay Basin. The ratio of mantle heat flow to surface heat flow in the Jizhong Depression was higher than those of the Linqing and Jiyang depressions during the Triassic and Jurassic.

However, the ratio of mantle heat flow to surface heat flow of the Jizhong Depression was lower than those of the other tectonic units in the Bohai Bay Basin, and has a present-day value of only 53%. Two peaks in the ratio of mantle heat flow to surface heat flow of the Jiyang Depression are higher than those of the other tectonic units. The ratio of mantle heat flow to surface heat flow of the Liaohe Depression reached an initial peak during the middle of the late Cretaceous, and the ratio was lower than those of the other tectonic units. The second peak in the ratio of the Liaohe Depression was comparable to those of other tectonic units in the Bohai Bay Basin.

There are also differences in the Moho temperature evolution between each unit of the Bohai Bay Basin. Moho temperatures of the Bohai Bay Basin reached an initial peak at the end of the early Cretaceous, except in the Liaohe Depression. Moho temperatures were relatively low in the Cangxian Uplift and Huanghua Depression, with temperatures of 940–960 °C, whereas Moho temperatures were greater than 980 °C in the other tectonic units in the basin. Moho temperatures reached their first peak of 970 °C during the middle of the late Cretaceous. The basin then experienced a low temperature phase at the end of the Cretaceous, and Moho

Table 5
Moho temperatures and heat flow partition of the Jizhong Depression during the Mesozoic and Cenozoic.

Time (Ma)	T_m (°C)	q_0 (mW/m^2)	q_m (mW/m^2)	q_c (mW/m^2)	q_m/q_0
240	645.8	54.56	25.99	28.57	47.6%
235	644.7	54.50	25.93	28.57	47.6%
230	644.7	54.50	25.93	28.57	47.6%
225	643.8	54.45	25.88	28.57	47.5%
220	643.8	54.45	25.88	28.57	47.5%
215	645.8	54.56	25.99	28.57	47.6%
210	645.8	54.56	25.99	28.57	47.6%
205	648.6	54.72	26.15	28.57	47.8%
200	651.2	54.87	26.30	28.57	47.9%
195	655.0	55.09	26.52	28.57	48.1%
190	656.8	55.19	26.62	28.57	48.2%
185	660.6	55.41	26.84	28.57	48.4%
180	665.2	55.67	27.10	28.57	48.7%
175	669.9	55.94	27.37	28.57	48.9%
170	674.4	56.20	27.63	28.57	49.2%
165	677.2	56.36	27.79	28.57	49.3%
160	683.7	56.73	28.16	28.57	49.6%
155	689.3	57.05	28.48	28.57	49.9%
150	695.7	57.42	28.85	28.57	50.2%
145	706.9	58.06	29.49	28.57	50.8%
140	716.2	58.59	30.02	28.57	51.2%
135	767.2	61.51	32.94	28.57	52.0%
130	778.0	66.87	35.50	31.37	53.1%
125	863.0	72.17	40.80	31.37	56.5%
120	935.4	76.68	45.31	31.37	59.1%
115	1010.0	81.30	49.93	31.37	61.4%
110	1058.1	84.33	52.96	31.37	62.8%
105	1082.7	85.86	54.50	31.36	63.5%
103	1084.4	85.97	54.60	31.37	63.5%
100	1074.2	85.33	53.96	31.37	63.2%
95	1025.7	82.31	50.94	31.37	61.9%
90	931.3	78.12	48.58	29.54	62.2%
85	869.5	74.08	44.54	29.54	60.1%
80	815.9	70.58	41.04	29.54	58.1%
75	774.5	67.88	38.34	29.54	56.5%
70	748.5	66.18	36.64	29.54	55.4%
65	736.3	65.38	35.84	29.54	54.8%
60	724.5	66.39	38.02	28.37	57.3%
55	758.3	68.72	40.35	28.37	58.7%
50	824.7	73.29	44.92	28.37	61.3%
45	786.0	79.97	58.24	21.73	72.8%
43	795.8	80.82	59.09	21.73	73.1%
40	787.9	80.13	58.40	21.73	72.9%
35	747.9	76.63	54.90	21.73	71.6%
30	704.3	72.81	51.08	21.73	70.2%
25	773.6	68.25	40.94	27.31	60.0%
20	758.9	64.27	37.53	26.74	58.4%
15	735.0	62.68	35.94	26.74	57.3%
10	715.0	61.35	34.61	26.74	56.4%
5	692.7	59.86	33.12	26.74	55.3%
0	635.3	57.74	33.39	24.35	53.0%

T_m, q_0, q_m, q_c and q_m/q_0 are referred to Table 2.

temperatures were relatively low (<740 °C) in the Cangxian Uplift, Linqing Depression, and Jizhong Depression. Moho temperatures in the other tectonic units were approximately 760 °C. The Bohai Bay Basin experienced a second peak in Moho temperatures, between 820 and 900 °C, which were significantly lower than the first Moho temperature peak.

Moho temperatures peaked a third time in the Linqing Depression, Cangxian Uplift, and Jizhong Depression, but the maximum temperature was significantly lower than those of the previous two peaks, reaching only 770–810 °C. Moho temperatures of the other depressions gradually deceased beginning in the late Paleogene, and these depressions did not experience a third peak in Moho temperatures. Presently, the highest Moho temperature exists in the Jiyang Depression (>680 °C), followed by the Cangxian Uplift and Linqing Depression. The lowest Moho temperature (<660 °C) is found beneath the Jizhong and Liaohe depressions.

Table 6
Moho temperatures and heat flow partition of the Huanghua Depression during the Mesozoic and Cenozoic.

Time (Ma)	T_m (°C)	q_0 (mW/m^2)	q_m (mW/m^2)	q_c (mW/m^2)	q_m/q_0
120	928.5	80.66	52.94	27.72	65.6%
115	940.7	81.51	53.79	27.72	66.0%
110	950.6	82.20	54.48	27.72	66.3%
107	955.2	82.52	54.80	27.72	66.4%
105	952.2	82.31	54.59	27.72	66.3%
100	931.7	80.88	53.16	27.72	65.7%
95	913.3	79.60	51.88	27.72	65.2%
90	932.9	78.22	48.68	29.54	62.2%
85	912.6	76.90	47.36	29.54	61.6%
80	893.1	75.62	46.08	29.54	60.9%
75	871.9	74.24	44.70	29.54	60.2%
70	849.3	72.76	43.22	29.54	59.4%
65	800.7	71.64	43.27	28.37	60.4%
60	805.4	71.96	43.59	28.37	60.6%
55	824.7	73.29	44.92	28.37	61.3%
50	847.0	74.83	46.46	28.37	62.1%
45	781.3	79.55	57.82	21.73	72.7%
40	833.4	84.11	62.38	21.73	74.2%
37	849.8	85.55	63.82	21.73	74.6%
35	846.7	85.28	63.55	21.73	74.5%
30	824.3	83.32	61.59	21.73	73.9%
25	869.4	71.64	44.90	26.74	62.7%
20	777.9	65.54	38.80	26.74	59.2%
15	755.6	64.05	37.31	26.74	58.2%
10	744.5	63.31	36.57	26.74	57.8%
5	737.3	62.83	36.09	26.74	57.4%
0	700.7	62.41	34.90	27.51	56.0%

T_m, q_0, q_m, q_c and q_m/q_0 are referred to Table 2.

6.2. Geodynamic evolution during the Mesozoic and Cenozoic

Understanding the lithospheric thermal structure enables preliminary interpretations of the Mesozoic and Cenozoic geodynamic evolution of the Bohai Bay Basin. The ratio of mantle heat flow to surface heat flow reveals that the Cretaceous represents a significant transitional period in the geological history of the basin. Significant tectonic activity in the upper mantle was accompanied by substantial crustal movement. The lithospheric thermal structure transformed from “cold mantle and hot crust” before the Cretaceous to “cold crust and hot mantle”. The ratio of mantle heat flow to surface heat flow exceeded 50% in the Cretaceous, particularly from the later part of the early Cretaceous to the Paleogene. During

Table 7
Moho temperatures and heat flow partition of the Liaohe Depression during the Mesozoic and Cenozoic.

Time (Ma)	T_m (°C)	q_0 (mW/m^2)	q_m (mW/m^2)	q_c (mW/m^2)	q_m/q_0
95	824.9	73.45	45.73	27.72	62.3%
90	862.9	76.10	48.38	27.72	63.6%
85	948.3	79.23	49.69	29.54	62.7%
80	969.4	80.61	51.07	29.54	63.4%
75	941.9	78.81	49.27	29.54	62.5%
70	894.0	75.68	46.14	29.54	61.0%
65	858.9	73.39	43.85	29.54	59.7%
60	832.4	73.82	45.45	28.37	61.6%
55	857.0	75.52	47.15	28.37	62.4%
50	883.9	77.37	49.00	28.37	63.3%
45	789.2	80.24	58.51	21.73	72.9%
40	818.9	82.84	61.11	21.73	73.8%
35	823.7	83.26	61.53	21.73	73.9%
30	795.2	80.77	59.04	21.73	73.1%
25	745.9	67.50	42.36	25.14	62.8%
20	673.1	62.20	37.06	25.14	59.6%
15	657.0	61.03	35.89	25.14	58.8%
10	647.5	60.34	35.20	25.14	58.3%
5	643.1	60.02	34.88	25.14	58.1%
0	662.8	59.70	34.60	25.10	58.0%

T_m, q_0, q_m, q_c and q_m/q_0 are referred to Table 2.

Table 8
Moho temperatures and heat flow partition of the Cangxian Uplift during the Mesozoic and Cenozoic.

Time (Ma)	T_m (°C)	q_0 (mW/m^2)	q_m (mW/m^2)	q_c (mW/m^2)	q_m/q_0
115	914.1	79.66	51.94	27.72	65.2%
110	927.1	80.56	52.84	27.72	65.6%
105	943.0	81.67	53.95	27.72	66.1%
100	936.3	81.20	53.48	27.72	65.9%
95	911.0	79.44	51.72	27.72	65.1%
90	907.7	76.58	47.04	29.54	61.4%
85	856.6	73.24	43.70	29.54	59.7%
80	810.2	70.21	40.67	29.54	57.9%
75	774.5	67.88	38.34	29.54	56.5%
70	749.2	66.23	36.69	29.54	55.4%
65	732.3	65.12	35.58	29.54	54.6%
60	722.2	66.23	37.86	28.37	57.2%
55	794.3	71.22	42.85	28.37	60.2%
50	890.8	77.85	49.48	28.37	63.6%
45	848.0	85.39	63.66	21.73	74.6%
40	852.8	85.81	64.08	21.73	74.7%
35	874.0	87.67	65.94	21.73	75.2%
30	773.4	78.86	57.13	21.73	72.4%
25	822.7	73.08	47.94	25.14	65.6%
20	766.4	68.99	43.85	25.14	63.6%
15	741.7	67.19	42.05	25.14	62.6%
10	724.9	65.97	40.83	25.14	61.9%
5	712.4	65.06	39.92	25.14	61.4%
0	730.0	64.48	39.33	25.15	61.0%

T_m, q_0, q_m, q_c and q_m/q_0 are referred to Table 2.

this period, two heat flow peaks occurred in the mantle, and the ratio of mantle heat flow to surface heat flow was greater than 65%.

According to previous studies (Hyndman et al., 1968; Lachenbruch, 1970; Chenbruch and Sass, 1977), the Australian Shield Moho temperature was 420 °C, the stable region of the eastern United States had a Moho temperature of 660 °C, and the Basin and Range Province in the western United States reached Moho temperatures of 860–1150 °C during Cenozoic tectonic activity. Therefore, we use 660 °C as the Moho temperature that distinguishes tectonically stable and active regions. Moho temperatures of the Bohai Bay Basin have exceeded 660 °C since the Cretaceous. In particular, temperatures reached 820–1100 °C during the late stages of the early Cretaceous to the Paleogene, and were maintained until the beginning of the Neogene. Subsequently, the Liaohe and Jizhong depressions underwent decreases in Moho temperatures to below 660 °C. Thus, the Bohai Bay Basin exhibited signs of tectonic activity during the Cretaceous and Paleogene. The Jizhong and Liaohe depressions gradually evolved into tectonically stable regions, whereas other areas in the basin fluctuated between tectonic stability and activity.

The Bohai Bay Basin experienced Yanshanian tectonism during the Jurassic to Cretaceous, including intense deformation and magmatic activity. Numerous fractures developed at the base of the crust and lithosphere (Xu et al., 2004), which caused significant magmatic and volcanic activity, including two large-scale magmatic events during the Jurassic–Cretaceous. Although Jurassic granite from the lithospheric mantle has been identified in the Bohai Bay Basin (Xu et al., 2004; Wu et al., 2005a,b), which implies asthenospheric upwelling in North China (Xu et al., 2009), the proportion of heat flow from the mantle increased. Moho temperature then increased and lithospheric thinning occurred. However, in terms of lithospheric thermal structure, this period marks the transition from structural stability to tectonic activity in the Bohai Bay Basin.

Compared with Jurassic magmatism, Cretaceous magmatism was significantly more extensive and voluminous. Mafic and silicic magmatism occurred simultaneously and mixed with mantle derived magmas, which formed I- to A-type granites (Xu et al., 2009). The northwestern extrusional stress field became the northwestern extensional stress field of eastern continental China. This may have been due to island arc subduction of the Kula Plate of the northern Pacific–Asia Pacific ridge, which is located at the eastern edge of the stress field. The Japan island arc was separated from the Asian continent due to tensile stress, and the Sea of Japan opened and connected with the East China Sea subsidence belt (Chen, 1988; Wang, 1996). During this period, a series of large-scale graben structures developed in the Bohai Bay Basin. The crustal thickness of the basin decreased due to isostatic adjustments, and a mantle arch and mantle uplift belt were formed. With crustal thinning and rifting, the mantle material upwelled, which resulted in increased mantle heat flow, elevated Moho temperatures, and large-scale magmatic activity, as well as a reduction in lithospheric thickness. This interpretation is consistent with the results of this study that indicate high surface heat flow, high mantle-to-surface heat flow ratios, high Moho temperatures, and thin lithosphere.

Rifting of the Bohai Bay Basin occurred again during the Paleogene. It was likely due to movement of material in the upper

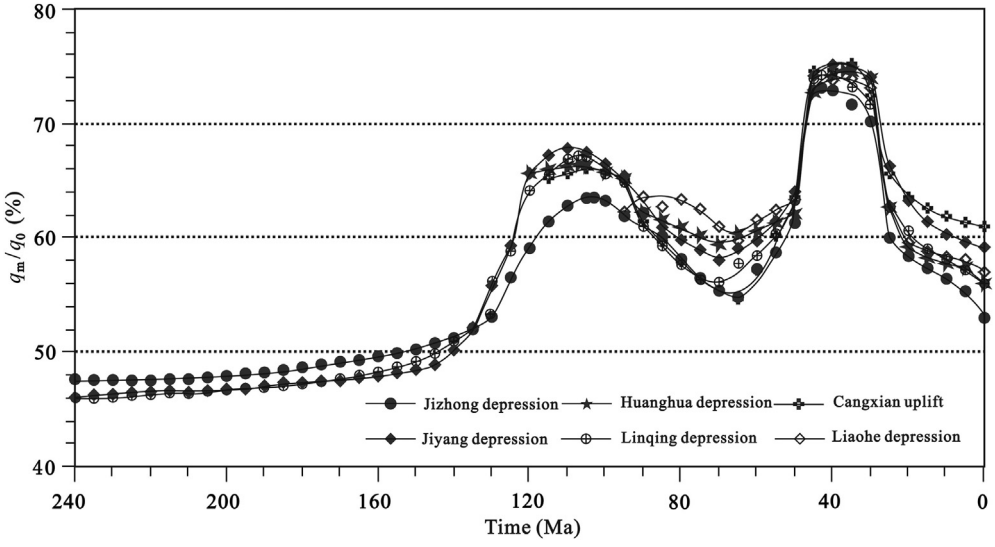

Figure 5. Ratio of the mantle heat flow to surface heat flow of the Bohai Bay Basin during the Mesozoic to Cenozoic.

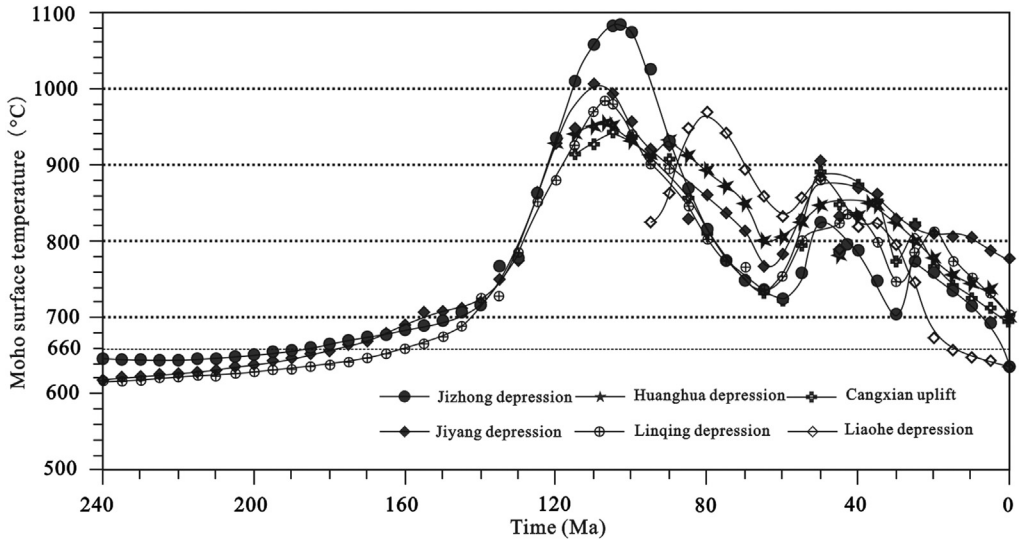

Figure 6. Moho temperatures of the Bohai Bay Basin during the Mesozoic to Cenozoic.

mantle, which led to uplift and stretching on both sides of the lithosphere. Subsequent lithospheric thinning was accompanied by large-scale magmatic activity, which is consistent with extensive occurrences of tholeiitic basalts. The direction of movement of the Pacific Plate changed significantly during the Paleogene to the early Neogene, and North China experienced strong compression in the ENE–WSW direction. Although some major uplift and depression belts existed, normal faulting continued, which was controlled by large-scale horst and graben structures. Depressions began to develop in the Bohai Bay Basin. The temperature of the basin began to decrease during the Neogene, as did magmatic activity and the related heat provided by the mantle upwelling. However, this period of decreasing temperatures was short-lived, as the Bohai Bay Basin currently exhibits a high thermal signature. Therefore, Moho temperatures and mantle heat flow remain high in the Bohai Bay Basin, suggesting that the thermal decay is ongoing.

7. Conclusions

Crustal and mantle heat flow partitioning and distribution, coupled with the evolution of Moho temperatures during the Mesozoic and Cenozoic, reveal that the Cretaceous represents a key period in the tectonic evolution of the Bohai Bay Basin. Intense thermal activity occurred in the upper mantle and crust, and lithospheric thermal structure transformed from a “cold mantle and hot crust” before the Cretaceous to a “hot mantle and cold crust” during and after the Cretaceous. The proportion of heat flow from the mantle has surpassed 50% of the surface heat flow since the Cretaceous, and Moho temperatures exceeded 660 °C. In particular, two mantle heat flow peaks occurred in the late stages of the early Cretaceous and Paleogene. During these peaks, the percentage of heat flow from the mantle was greater than 65% of the surface heat flow. Three Moho temperature peaks occurred in the early Cretaceous (900–1100 °C), Paleogene (820–900 °C), and (in the Linqing Depression, Cangxian Uplift, and Jizhong Depression) early Neogene (770–810 °C). The lithospheric thermal structure in the Bohai Bay Basin indicates that the region was relatively tectonically stable during the Triassic and Jurassic. The region subsequently became tectonically active during the Cretaceous and Paleogene, and fluctuated between tectonic activity and stability in the late Cretaceous. The Jizhong and Liaohe depressions gradually transformed into stable tectonic zones, which they continue to be today. The rest of the basin continues to vary from tectonically stable to active.

Acknowledgements

Two anonymous reviewers are thanked for their reviews that greatly improved this paper. This work was funded by the National Natural Science Foundation of China (Grant Nos. 41402219, 41302202, 41125010, 41302202, and 91114202).

References

Ashchepkov, I.V., Rotman, A.Y., Somov, S.V., Afanasiev, P., Downes, H., Logvinova, A.M., Nossyko, S., Shimupi, J., Palessky, S.V., Khmelnikova, O.S., Vladykin, N.V., 2012. Composition and thermal structure of the lithospheric mantle beneath kimberlite pipes from the Catoca cluster, Angola. Tectonophysics 530–531, 128–151.

Baumann, M., Rybach, L., 1992. Temperature field modeling along the northern segment of the European geotraverse and the Danish transition zone. Tectonophysics 194, 387–407.

Birch, F., Roy, R.F., Decker, E.R., 1968. Heat flow and thermal history in New York and New England. In: Zen, E., Wtite, W.S., Hadley, J.B., Thompson Jr., J.B. (Eds.), Studies of Applachian Geology, Northern and Maritime. Interscience, New York, pp. 437–451.

Blackwell, D.D., 1971. The thermal structure of the continental crust. In: Heaoock, J.G. (Ed.), The Structure and Physical Properties of the Earth Crust. AGU, pp. 169–184.

Bruno, G., 2010. Combining seismically derived temperature with heat flow and bathymetry to constrain the thermal structure of oceanic lithosphere. Earth and Planetary Science Letters 295, 390–400.

Cai, X.L., Zhu, J.S., Cao, J.M., Cheng, X.X., 2007. 3D structure and dynamic types of the lithospheric crust in continental China and its adjacent regions. Geology in China 34, 544–557 (in Chinese).

Cermak, V., Bodri, L., 1986. Two–dimensional temperature modeling along five East–European geotraverses. Journal of Geodynamics 5, 133–163.

Chen, L., 2009. Lithospheric structure variations between the eastern and central North China Craton from S-and P-receiver function migration. Physics of the Earth and Planetary Interiors 173, 216–227.

Chen, L., Tao, W., Zhao, L., Zheng, T.Y., 2008. Distinct lateral variation of lithospheric thickness in the Northeastern North China Craton. Earth and Planetary Science Letters 267, 56–68.

Chen, L., Zheng, T.Y., Xu, W.W., 2006. A thinned lithospheric image of the Tanlu Fault Zone, eastern China: constructed from wave equation based receiver function migration. Journal of Geophysical Research 111. http://dx.doi.org/10.1029/2005JB003974. B09312.

Chen, M.X., 1988. North China Geothermy. Science Press, Beijing (in Chinese).

Chenbruch, A.H., Sass, J.H., 1977. Heat flow in the United States and the thermal regime of the crust. In: Spilhaus, A.F., Managing, J. (Eds.), The Earth’s Crust, its Nature and Physical Properties, Geophysical Monograph, vol. 20, pp. 332–359.

Cooper, C.M., Lenardic, A., Moresi, L., 2004. The thermal structure of stable continental lithosphere within a dynamic mantle. Earth and Planetary Science Letters 222, 807–817.

Dmitrienko, L.V., Li, S.Z., Cao, X.Z., Suo, Y.H., Wang, Y.M., Dai, L.M., Somerville, I.D., 2016. Large-scale morphotectonics of the ocean-continent transition zone between the western Pacific Ocean and the east Asian Continent: a link of deep process to the Earth's surface system. Geological Journal 51, 263–285. http://dx.doi.org/10.1002/gj.2845.

Gong, Y.L., 2003. The Thermal Structure and Thermal Evolution of Bohai Bay Basin in East China (dissertation). Nanjing University, Nanjing (in Chinese with English abstract).

Gong, Y.L., Wang, L.S., Liu, S.W., Li, C., Han, Y.B., Li, H., Cai, J.G., 2005. Mantle heat flow and deep temperature of Jiyang depression, Sangdong, north China. Earth Science–Journal of China University of Geosciences 30, 121–128 (in Chinese with English abstract).

Gornov, M.V., Goroshko, Y.F., Malyshev, Y., Podgornyi, Y., 2009. Thermal structure of lithosphere in central Asian and Pacific belts and their adjacent cratons from data of geoscience transects. Russian Geology and Geophysics 50, 485–499.

He, L.J., 2015. Thermal regime of the North China Craton: implications for craton destruction. Earth-Science Reviewers 140, 14–26.

He, L.J., Hu, S.B., Wang, J.Y., 2001. Lithospheric thermal structure characteristic in the eastern China Continent. Progress in Natural Science 11, 966–969 (in Chinese with English abstract).

Hou, G.T., Qian, X.L., Cai, D.S., 2001. The tectonic evolution of Bohai basin in Mesozoic and Cenozoic time. Acta Scientiarum Naturalium Universitatis Pekinensi 37, 845–851 (in Chinese with English abstract).

Hu, S.B., Paul, B.O.S., Asaf, R., 2001. Thermal history and tectonic subsidence of the Bohai Basin, northern China: a Cenozoic rifted and local pull–apart basin. Physics of the Earth and Planetary Interiors 126, 221–235.

Hu, S.B., Wang, J.Y., 1994. Crustal heat production and mantle heat flow in Southeast China. Science in China 37, 1252–1263 (in Chinese).

Hyndman, R.D., Lambert, I.B., Heier, K.S., Jaeger, J.C., Ringwood, A.E., 1968. Heat flow and surface radioactivity measurement in the Precambrian shield of western Australia. Physics of the Earth and Planetary Interiors 1, 128–135.

Jaupart, C., Mareschal, J.C., 2014. Lithosphere, continental: thermal structure. In: Encyclopedia of Solid Earth Geophysics. Springer, Netherlands, pp. 681–693.

Ji, Y.L., Hu, G.M., Huang, J.J., Wu, Z.P., 2006. Eroded strata thickness of mesozoic and evolution of Mesozoic and Cenozoic Basins in the Bohai Bay Basin area. Acta Geologica Sinica 80, 351–358 (in Chinese with English abstract).

Ketcham, R.A., 1996. Distribution of heat producing elements in the upper and middle crust of southern and west central Arizona: evidence from the core complex. Journal of Geophysical Research 101, 13611–13632.

Lachenbruch, A.H., 1970. Crustal temperature and heat production, implication of the linear heat flow relation. Journal of Geophysical Research 75, 3291–3300.

Laslett, G.M., Green, P.F., Duddy, I.R., Gleadow, A.J.W., 1987. Thermal annealing of fission tracks in apatite, 2. A quantitative analysis. Chemical Geology 65, 1–13.

Lerche, I., 1998. Inversion of multiple thermal indicators: quantitative methods of determining paleoheat flux and geological parameters, 1. Theoretical development for paleoheat flux. Mathematical Geology 20, 3–36.

Li, S.Z., Suo, Y.H., Santosh, M., Dai, L.M., Yu, S., Zhao, S.J., Jin, C., 2013. Mesozoic to cenozoic intracontinental dynamics of the north China block. Geological Journal 48 (5), 543–560.

Li, S.Z., Zhao, G.C., Dai, L.M., Liu, X., Zhou, L.H., Santosh, M., Suo, Y.H., 2012a. Mesozoic basins in eastern China and their bearings on the deconstruction of the North China Craton. Journal of Asian Earth Sciences 47, 64–79.

Li, S.Z., Zhao, G.C., Dai, L.M., Zhou, L.H., Liu, X., Suo, Y.H., Santosh, M., 2012b. Cenozoic faulting of the Bohai Bay Basin and its bearings on the destruction of the eastern North China Craton. Journal of Asian Earth Sciences 47, 80–93.

Liu, G.D., 1987. The Cenozoic rift system of the North China plain and the deep internal process. Tectonophysics 133, 277–285.

Liu, Q.Y., He, L.J., Huang, F., Zhang, L.Y., 2016. Cenozoic lithospheric evolution of the Bohai Bay Basin, eastern North China Craton: constraint from tectono-thermal modeling. Journal of Asian Earth Sciences 115, 368–382.

Liu, S.W., Wang, L.S., Gong, Y.L., Li, C., Li, H., Han, Y.B., 2005. Lithospheric thermal–rheological structure and their geodynamic significance in the Jiyang depression. Science in China (Ser. D) 35, 203–214 (in Chinese).

Mall, D.M., Sharma, S.R., 2009. Tectonics and thermal structure of western Satpura, India. Journal of Asian Earth Sciences 34, 450–457.

McLennan, S.M., Taylor, S.R., 1996. Heat flow and the chemical composition of continental crust. The Journal of Geology 104, 369–377.

Nathan, L.G., 2006. Influence of slab thermal structure on basalt source regions and melting conditions, REE and HFSE constraints from the Garibaldi volcanic belt, northern Cascadia subduction system. Lithos 87, 23–49.

Pasquale, V., Cabella, C., Verdoya, M., 1990. Deep temperatures and lithospheric thickness along the European geotraverse. Tectonophysics 176, 1–11.

Peng, B., Zou, H.Y., 2013. Present–day geothermal structure of lithosphere and the Cenozoic tectono-thermal evolution of Bohai Basin. Geoscicences 27, 1399–1406 (in Chinese with Enligh abstract).

Qiu, N.S., 1998. Thermal status profile in terrestrial sedimentary basins in China. Advance in Earth Sciences 13, 447–451 (in Chinese with English abstract).

Qiu, N.S., Xu, W., Zuo, Y.H., Chang, J., 2015a. Meso–cenozoic thermal regime in the Bohai Bay Basin, eastern North China Craton. International Geology Review 57 (3), 1–19.

Qiu, N.S., Xu, W., Zuo, Y.H., Chang, J., 2015b. Meso–cenozoic thermal regime in the Bohai Bay Basin, eastern North China Craton. International Geology Review 57, 271–289.

Qiu, N.S., Zuo, Y.H., Chang, J., Li, W.Z., 2014. Geothermal evidence of the Mesozoic and Cenozoic lithospheric thinning in the Jiyang depression. Gondwana Research 26, 1079–1092.

Rao, S., Hu, S.B., Zhu, C.Q., Tang, X.Y., Li, W.W., Wang, J.Y., 2013. The Characteristics of heat flow and lithospheric thermal structure in Junggar Basin, northwest China. Chinese Journal of Geophysics 56, 2760–2770 (in Chinese with Enligh abstract).

Rudnick, R.L., McDonough, W.F., O'Connell, R.J., 1998. Thermal structure, thickness and composition of continental lithosphere. Chemical Geology 145, 395–411.

Shao, J.A., Lu, F.X., Zhang, L.Q., Yang, J.H., 2005. Discovery of xenocrysts in basalts of Yixian formation in west Liaoning Province and its significance. Acta Petrologica Sinica 211, 547–1558 (in Chinese with English abstract).

Sweeney, J.J., Burnham, A.K., 1990. Evaluation of a simple model of vitrinite reflectance based on chemical kinetics. AAPG Bulletin 74, 1559–1571.

Tian, K.Q., Yu, Z.H., Feng, M., 2000. Eogene Deep Oil and Gas Geology and Exploration in the Bohai Bay Basin. Petroleum Industry Press, Beijing (in Chinese).

Wang, J.Y., 1996. Geothermics in China. Seismological Press, Beijing (in Chinese).

Wang, Y., Cheng, S.H., 2012. Lithospheric thermal structure and rheology of the eastern China. Journal of Asian Earth Sciences 47, 51–63.

William, P.L., Jared, F.L., Russell, C.E., Richard, M.C., Martin, J.S., 2005. Evarts, petrologic constraints on the thermal structure of the Cascades arc. Journal of Volcanology and Geothermal Research 140, 67–105.

Wu, F.Y., Li, X.H., Yang, J.H., Zheng, Y.F., 2007. Discussions on the petrogenesis of granites. Acta Petrologica Sinica 23, 1217–1238 (in Chinese with English abstract).

Wu, F.Y., Lin, J.Q., Wilde, S.A., Zhang, X.O., Yang, J.H., 2005b. Nature and significance of the Early Cretaceous giant igneous event in eastern China. Earth and Planetary Science Letters 233, 103–119.

Wu, F.Y., Yang, J.H., Wilde, S.A., Zhang, X.O., 2005a. Geochronology, petrogenesis and tectonic implications of Jurassic granites in the Liaodong Peninsula, NE China. Chemical Geology 221, 127–156.

Xu, P.F., Zhao, D.P., 2009. Upper–mantle velocity structure beneath the North China Craton, implications for lithospheric thinning. Geophysical Journal International 177, 1279–1283.

Xu, Y.G., Li, H.Y., Pang, C.J., He, B., 2009. On the timing and duration of the destruction of the North China Cration. Chinese Science Bulletin 54, 1974–1989.

Xu, W.L., Wang, Q.H., Wang, D.Y., Pei, F.P., Gao, S., 2004. Processes and mechanism of Mesozoic lithospheric thinning in eastern North China Craton: evidence from Mesozoic igneous rocks and deep–seated xenoliths (in Chinese). Earth Science Frontiers 3, 309–317 (in Chinese with English abstract).

Zang, S.X., Liu, Y.G., Ning, J.Y., 2002. Thermal structure of the lithosphere in north China. Chinese Journal of Geophysics 45, 56–66 (in Chinese with English abstract).

Zhai, M.G., Fan, Q.C., Zhang, H.F., Sui, J.L., 2005. Lower crust processes during the lithosphere thinning in eastern China: magma underplating, replacement and delamination. Acta Petrologica Sinica 21, 1509–1526 (in Chinese with English abstract).

Zhang, H.F., Yang, Y.H., 2007. Emplacement age and Sr-Nd-Hf isotopic characteristics of the diamondiferous kimberlites from the eastern North China Craton. Acta Petrologica Sinica 23, 285–294 (in Chinese with English abstract).

Zhu, G., Hu, S.Q., Chen, Y., 2008. Evolution of Early Cretaceous extensional basins in the eastern North China Craton and its implication for the craton destruction. Geological Bulletin of China 20, 1594–1604 (in Chinese with English abstract).

Zhu, R.X., Chen, L., Wu, F.Y., Liu, J.L., 2011. Timing, scale and mechanism of the destruction of the North China Craton. Science China Earth Sciences 54, 789–797.

Zhu, R.X., Yang, J.H., Wu, F.Y., 2012. Timing of destruction of the North China Craton. Lithos 149, 51–60.

Zuo, Y.H., Qiu, N.S., Pang, X.Q., Chang, J., Hao, Q.Q., Gao, X., 2013. Geothermal evidence of the Mesozoic and Cenozoic lithospheric thinning in the Liaohe depression. Journal of Earth Science 24, 529–540.

Zuo, Y.H., Qiu, N.S., Li, J.W., Hao, Q.Q., Pang, X.Q., Zhao, Z.Y., Zhu, Q., 2015. Meso–Cenozoic tectono–thermal evolution history in Bohai Bay Basin, north China. Journal of Earth Science 26, 352–360.

Zuo, Y.H., Qiu, N.S., Zhang, Y., Li, C.C., Li, J.P., Guo, Y.H., Pang, X.Q., 2011. Geothermal regime and hydrocarbon kitchen evolution of the offshore Bohai Bay Basin, North China. AAPG Bulletin 95, 749–769.

Zuo, Y.H., Wang, C.C., Tang, S.L., Hao, Q.Q., 2016. Mesozoic and Cenozoic thermal history and source rock thermal evolution of the Baiyinchagan Sag, Erlian Basin, Northern China. Journal of Petroleum Science and Engineering 139, 171–184.